

High-energy thermal study of the high-entropy silver–copper alloy system using the PBIN database and Thermo-Calc software package

W.U. Shah,^{1,*} D.F. Khan,¹ J.S. Shah,² H.Q. Yin³ and A.G. Mamalis⁴

¹ *Department of Physics, University of Science and Technology, Bannu 28100, Khyber Pukhtunkhuwa, Pakistan*

² *Department of Physics, Islamia College, University of Peshawar, Pakistan*

³ *School of Materials Science and Engineering, University of Science and Technology, Beijing 100083, P.R. China*

⁴ *Project Centre for Nanotechnology and Advanced Engineering (PC-NAE), NCSR “Demokritos”, Athens, Greece*

High-energy thermal analysis using the CALPHAD method has been undertaken to determine the phase diagram, Gibbs energy, enthalpy, thermodynamic molar activities and excess energies at temperatures of 1800 K, 1850 K and 1900 K at a constant atmospheric pressure of 10^6 Pa. The Ag–Cu system shows the highest positive deviations from Henry’s and Vegard’s laws at 1850 K, due to a high level of repulsive contacts; at this temperature the total Gibbs energy of the system also has its highest value, -6.609 MJ/mol. The alloy shows a good negative deviation from Raoult’s law, indicating system stability at the highest enthalpy level (again at 1850 K). The alloy is therefore shown to be usefully stable for industrial use.

1. Introduction

High-entropy alloys have a great ability to mix with other alloying elements, hence the properties of these composite systems can easily be modified.^{1,2} For novel production technologies, including those involving thermochemical treatment and spray forming, high-entropy alloys perform well. Up to the 1970s materials processing possibilities were limited; to remove some of those limitations, high-entropy alloys were formulated. The key principle is the high entropy of

* Corresponding author. E-mail address: waseemullahshah303@gmail.com

¹ J.C.M. Li (ed.), *Microstructure and Properties of Materials*, vol 1. Singapore: World Scientific (1996).

² Jien-Wei Yeh et al., Nanostructured high-entropy alloys with multiple principal elements: Novel alloy design concepts and outcomes. *Adv. Engng Mater.* **6** (2004) 299–303.

mixing, which is considered to be the most important feature for the formulation and making of multielement solid solution-based phases (which may include intermetallic compounds).³

Metastable alloys present challenging phase transformations. The CALPHAD (calculation of phase diagrams) method facilitates the thermodynamic analysis of alloys and is especially suitable for binary and ternary systems. The key equation for the total Gibbs energy G is:⁴

$$G = G_{\text{Ag}}x_{\text{Ag}} + G_{\text{Cu}}x_{\text{Cu}} + k_{\text{B}}T(x_{\text{Ag}}L_{\text{Ag}} + x_{\text{Cu}}L_{\text{Cu}}) + G_{\text{ex}} \quad (1)$$

where G_{Ag} and G_{Cu} are the Gibbs energies of the pure metal, x_{Ag} and x_{Cu} the atom fractions of each component, k_{B} is Boltzmann's constant, T the temperature, L_{Ag} and L_{Cu} are parameters representing the angular symmetry of each atom, and G_{ex} is the excess Gibbs energy of mixing.

For the Ag–Cu system, the equilibrium complexes and temperature boundaries need to be carefully addressed (the eutectic behaviour of the Ag–Cu solid solution has been previously studied⁵). The present paper reveals the heterogeneity of the system and the enthalpy of formation cascades by removing some limitations of the CALPHAD method.⁶

We used the Thermo-Calc software for calculation of the thermodynamic quantities of the alloy system. The Miedema model is a useful adjunct to the CALPHAD method in the case of metastable binary alloys such as Ag–Cu, composed of Wigner–Seitz (WS) cells, because of the lack of equilibrium. As the pure metal becomes adulterated, the WS cell geometry changes. Two influences then supervene: the electronegativity difference of the constituent elements and the diminishing electron density between components after mixing, yielding a positive mixing enthalpy contribution.⁷

2. Procedure

For liquid binary alloys and solid solutions the excess enthalpy of disorder $(\Delta H_{\text{Ag,Cu}})_{\text{disorder}}$ is calculated as:^{7a}

$$(\Delta H_{\text{Ag,Cu}})_{\text{disorder}} = f_{\text{Ag,Cu}}x_{\text{Ag}}[1 + u_{\text{Ag}}x_{\text{Cu}}(\Phi_{\text{Ag}} - \Phi_{\text{Cu}})]x_{\text{Cu}}[1 + u_{\text{Cu}}x_{\text{Ag}}(\Phi_{\text{Cu}} - \Phi_{\text{Ag}})] / \{x_{\text{Ag}}V_{\text{Ag}}^{2/3}[1 + u_{\text{Ag}}x_{\text{Cu}}(\Phi_{\text{Ag}} - \Phi_{\text{Cu}})] + x_{\text{Cu}}V_{\text{Cu}}^{2/3}[1 + u_{\text{Cu}}x_{\text{Ag}}(\Phi_{\text{Cu}} - \Phi_{\text{Ag}})]\} \quad (2)$$

where $f_{\text{Ag,Cu}}$ is the alloying activity of interaction^{7a} (with parameters obtained from⁸), Φ are electronegativities, V are the Helmholtz potentials during alloying and the u are empirical parameters obtained by fitting to known data. For ordered intermetallic components, we have:^{7a}

$$(\Delta H_{\text{Ag,Cu}})_{\text{order}} = \Delta H_{\text{Ag,Cu}}[1 + 8\Delta H_{\text{Ag,Cu}}^{2/3} / \{f_{\text{Ag,Cu}}(x_{\text{Ag}}V_{\text{Ag}}^{2/3}[1 + u_{\text{Ag}}x_{\text{Cu}}(\Phi_{\text{Ag}} - \Phi_{\text{Cu}})] + x_{\text{Cu}}V_{\text{Cu}}^{2/3}[1 + u_{\text{Cu}}x_{\text{Ag}}(\Phi_{\text{Cu}} - \Phi_{\text{Ag}})]\}^2]. \quad (3)$$

³ Jien-Wei Yeh, Recent progress in high-entropy alloys. *Eur. J. Control* **31** (2006) 633–682.

⁴ Xiuqing Li, A.P. Miodownik, N. Saunders, Simultaneous calculations of mechanical properties and phase equilibria. *J. Phase Equilibria* **22** (2008) 247–253; N. Saunders, A.P. Miodownik (eds), *CALPHAD (Calculation of Phase Diagrams): A Comprehensive Guide*, vol. 1. Elsevier (1998).

⁵ K.A. Gschneidner, J.-C. Bünzli and V.K. Pecharsky (eds), *Handbook on the Physics and Chemistry of the Rare Earths*, vol. 33. Elsevier (2003).

⁶ W.-F. Ho, W.-K. Chen, S.-C. Wu, H.-C. Hsu, Structure, mechanical properties, and grindability of dental Ti–Zr alloys, *J. Mater. Sci. Mater. Med.* **19** (2008) 3179–3186.

⁷ W.C. Wang, J.H. Li, H.F. Yan and B.X. Liu, A thermodynamic model proposed for calculating the standard formation enthalpies of ternary alloy systems. *Scr. Mater.* **56** (2007) 975–978.

^{7a} Haihong Li, Xueqin Sun and Shangzhou Zhang, Calculation of thermodynamic properties of Cu–Ce binary alloy and precipitation behavior of Cu₅Ce phase. *Mater. Trans.* **55** (2014) 1816–1819.

⁸ S. Sheibani, S. Heshmati-Manesh and A. Ataie, Structural investigation on nano-crystalline Cu–Cr supersaturated solid solution prepared by mechanical alloying, *J. Alloys Compounds* **495** (2010) 59–62.

3. Results

3.1 Phase diagram

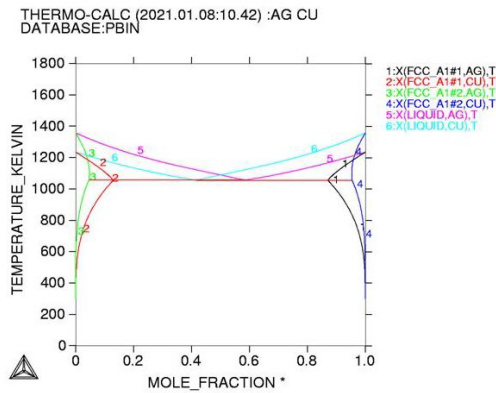


Figure 1. Computed phase diagram of the Ag–Cu alloy (colour online), showing face-centred cubic (FCC) and liquid phases. The abscissa gives x_{Cu} , the fraction of Cu atoms in the alloy.

Fig. 1 shows the phase diagram of the silver–copper binary system obtained by the CALPHAD method (Thermo-Calc package). The system shows three metastable phases. At 1850 K the highest stable and surviving phase is a liquid one with composition range 0.2–0.45. A further temperature increase results in the same liquid phase. The magnetic ferrite phase FCC_A1 is seen at temperatures below 900 K. The FCC_A1#2 phase is found in the temperature range 200–1090 K with a composition range of 0.0–0.06 mol. The liquid state is stable up to a high temperatures range (1090–1900 K). The phase boundaries are sharp.

3.2 The liquid phase

Using the four-species association model,^{9,10} the Gibbs free energy of the liquid phase is approximately:^{10a}

$$G_m^{\text{liquid}} = x_{AgCu}^0 G_{AgCu}^{\text{liquid}} + RT x_{AgCu} \ln x_{AgCu} + x_{AgCu} x_{CuAg}^0 L_{AgCu}^{\text{liquid}} \quad (4)$$

with L_{AgCu}^{liquid} an empirical interaction parameter to be evaluated from data. By only considering pairwise interaction between species, the Gibbs energy of the Ag–Cu atom-pairs simplifies to:^{10a}

$$G_{AgCu}^{\text{liquid}} = G_{Ag}^{\text{liquid}} + G_{Cu}^{\text{liquid}} + \Delta G_{AgCu}^{\text{liquid}} \quad (5)$$

and this expression can be substituted into eqn (4) to give the Gibbs free energy of liquid alloy formation.

⁹ M. Turchanin, P. Agraval, L. Dreval and A. Vodopyanova, Calorimetric investigation of the mixing of enthalpy of liquid Hf–Ni–Ti alloys and thermodynamic properties and chemical ordering in quaternary liquid Cu–Hf–Ni–Ti alloys. *J. Phase Equilibria Diffusion* **41** (2020) 469–490 .

¹⁰ K. Ozturk, L.Q. Chen and Z.K. Liu, Thermodynamic assessment of the Al–Ca binary system using random solution and associate models. *J. Alloys Compounds* **340** (2002) 199–206.

^{10a} Shihuai Zhou, Yi Wang, F.G. Shi, F. Sommer, Long-Qing Chen, Zi-Kui Liu and R.E. Napolitano, Modeling of thermodynamic properties and phase equilibria for the Cu–Mg binary system. *JPEDAV* **28** (2007) 158–166.

3.3 Terminal FCC phases

These phases are found by using a substitution solution model and treating them as a simple binary alloy.^{10a,11}

4. Results and discussion

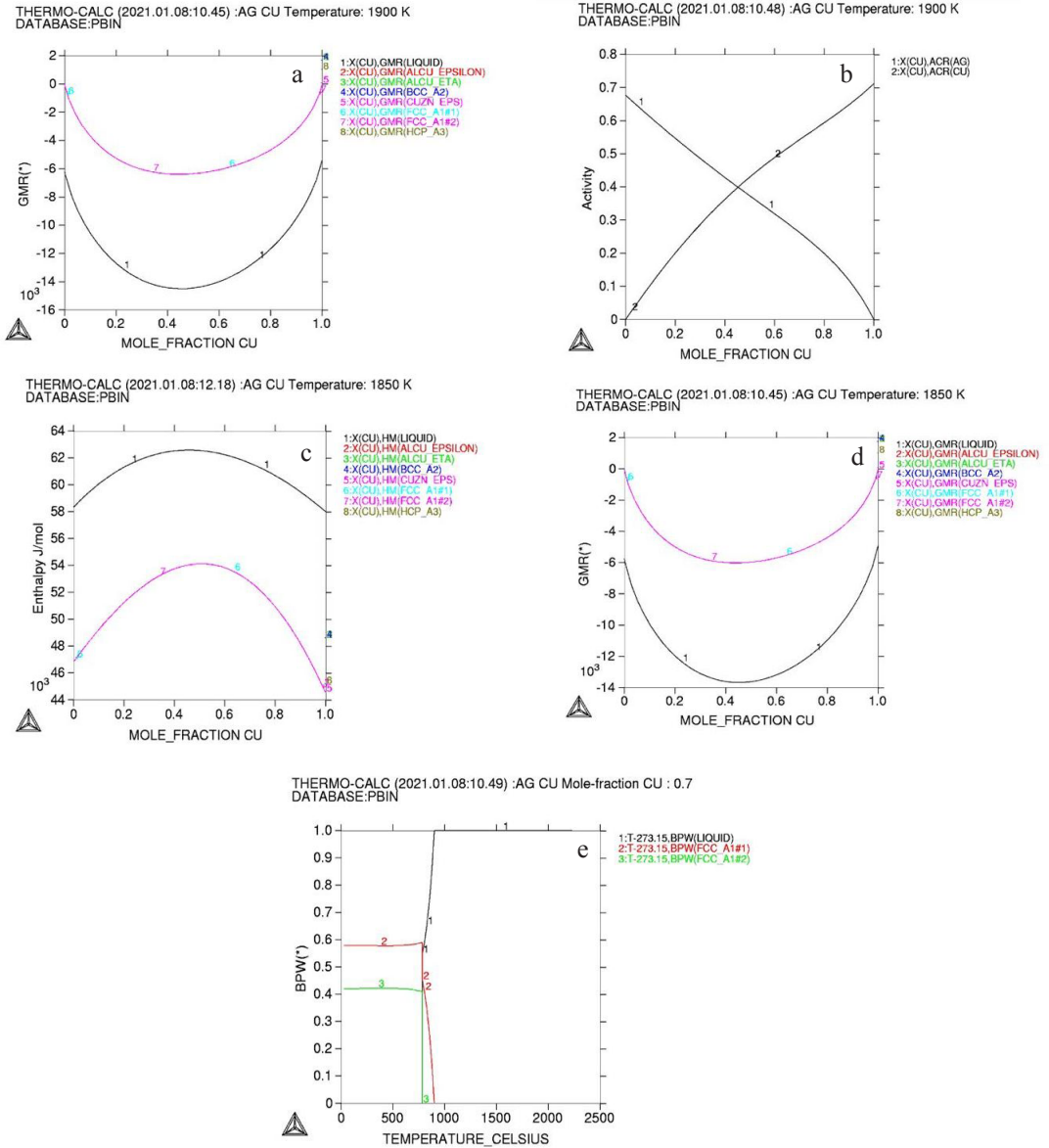


Figure 2. Calculated thermodynamic properties (see text; colour online), including (*) relative Gibbs energy (GMR) and (*) mass fractions for stable phases (BPW).

¹¹ H. Lüth, *Surfaces and Interfaces of Solid Materials* (6th edn). Springer (2015).

Fig. 2 shows total Gibbs energy, thermodynamic molar activity, enthalpy and mole fraction of the Ag–Cu binary alloy system. The Gibbs free energy was calculated through simulations at temperatures 1800–1900 K. It seems that the liquid régime is the most temperature-stable. The austenite and ferrite phases seem less stable. Activity shows a positive deviation from Vegard's and Henry's laws. This shows increasing enthalpy. A corresponding positive deviation from Raoult's law is seen, which indicates repulsive interaction among the alloying elements and implies less epitaxial growth of the alloying system.

Table 1. High-energy thermodynamic attributes of the Ag–Cu system at three different temperatures (pressure kept constant at 106 Pa).

T/K	N^a	ACRX ^b	M /kg ^c	G^d /MJ mol ⁻¹	V /mm ³	Enthalpy /MJ mol ⁻¹	SER ^e activity Ag	SER ^e activity Cu
1800	76.5	0.7, 0.3	7.24	-10.03	0.01	4.63	53.58, 79.84	22.96, 20.16
							1.2676×10^{-4}	2.5866×10^{-4}
							-1.343×10^5	-1.2363×10^5
LIQUID#1	76.5	--	7.24	--	--	--	0.798	0.202
1850	48.4	0.7,0.3	4.58	-6.61	0.01	3.01	33.91, 79.84	14.53, 20.15
							1.139×10^{-4}	2.2980×10^{-4}
							-1.397×10^5	-1.2887×10^5
LIQUID#1	48.4	--	4.58	--	--	--	0.7984	0.2016
1900	2.28		0.216	-0.324	--	0.146	1.5976	6.8467810^{-1}
		--					7.9842×10^{-1}	2.0158×10^{-1}
							1.0254810^{-4}	2.049×10^{-4}
							-1.452×10^5	-1.342×10^5
LIQUID#1	2.28	--	0.216	--	--	--	0.7984	0.2016

^a Number of moles. ^b Component proportions (Ag,Cu). ^c Mass. ^d Total Gibbs energy. ^e Stable element reference state.

Table 1 gives the results of the thermodynamic calculations. The molar mass of the alloying elements changes as the temperature increases and activity increases with a corresponding decrease of Gibbs total energy that shows stability of the system. The peak negative deviation is observed at 1850 K. Increasing stability implies hardening, wear resistance, corrosion resistance *inter alia*. At 1900 K the surviving phase is again LIQUID#1. According to the calculation the highest stability and hence most likely application in industry is at 1800 K.

5. Conclusions

No equilibrium is found in the investigated alloy system, which accordingly displays a metastable nature. With increasing temperature, the enthalpy of the system gradually increases due to repulsion forces among the alloying elements. Deviations from Vegard's and Henry's

laws are positive, in accordance with previous literature. Nevertheless, the alloy still shows stability, as evinced by decreasing Gibbs energy with increasing enthalpy. Deviation from Raoult's law is negative. The total Gibbs energy of the Ag–Cu system decreases with increasing temperature, indicating its stability. This implies hardening, wear resistance, corrosion resistance and other valuable characteristics. We observed maximum enthalpy at 1850 K. Overall, our results demonstrate the system's complex nature and are useful not only as a basis for further research but also for actual industrial applications.